

The Simulation of APM Operations: A Case Study of Suvarnabhumi Airport

Taksaporn Thongboonpian¹, Waressara Weerawat^{1,*}, and Norio Tomii²

¹ Department of Industrial Engineering, Faculty of Engineering, Mahidol University, Nakhon Pathom, Thailand

² College of Industrial Technology, Nihon University, Japan

Email: taksapornnui@gmail.com (T.T.); waressara.wee@mahidol.edu (W.W.); tomii.norio@nihon-u.ac.jp (N.T.)

*Corresponding author

Abstract—For the first time in Thailand, an Automated People Mover (APM) has been implemented at Suvarnabhumi Airport. The APM uses the guided way concept similar to metro rail operations, but with driverless trains on rubber wheels. As the APM becomes a key transport technology especially for large airports, it is worth investigating the operations to ensure service viability of driverless APM operations. This research uses a microscopic simulation model to evaluate the feasibility of APM operations and timetables in accordance with capacity requirements. The APM headway is often limited by turn-back operations using a single track at the entry-exit of the station. To increase line capacity, headway should be decreased or train capacity should be increased and the itinerary needs to be reevaluated. For an airport APM, the headway should only be decreased within certain limits to achieve the benefits of higher network capacity without compromising passenger travelling time. Increasing train capacity using coupled trains can accommodate more passengers on each trip, but the number of trains available should be considered. The simulation result reveals the critical factors that contribute to improve network capacity and offers guidance for the complex APM operations in the future.

Keywords—Automated People Mover (APM), timetable, simulation, airport transit

I. INTRODUCTION

The world's aviation industry has grown rapidly in the past two decades. In 2006, Suvarnabhumi also known as Bangkok Airport, officially became Thailand's main international airport in place of the former Don Mueang Airport which had been in use since 1914. With plans to handle up to 45 million passengers per year, the new Bangkok airport unexpectedly reached its design capacity in just five years. In 2019, Bangkok Airport ranked among the top 20 busiest airports in the world with around 65 million passengers per year [1]. The capacity of the airport needs to accommodate the increased number of passengers. Areas and facilities have been added to accommodate 120 million passengers per year. To transport passengers in the expanded airport area, an

Automated People Mover (APM) was implemented in September 2023 after some delays mainly due to COVID-19. It is the first time that an APM has been used at any airport in Thailand. Therefore, in order to ensure efficiency in service, it is essential to have a systematic plan for APM operations that aligns with the number of passengers in each period. This is particularly important for 24-hour service operations.

The APM system is an automated driverless transit system operated on a fixed guideway infrastructure [2]. It has the benefit of transporting a high volume passengers in a short period of time, increasing convenience in boarding and alighting without interfering with the aircraft taxiway. The system has fully automated vehicles running on a guideway. Each vehicle is equipped with special communications equipment to allow safe driverless operation with Automatic Train Protection (ATP) similar to modern rail transit systems. The vehicle positions for the entire network are controlled from the Operations Control Center (OCC). The train separation function of the signaling systems used in the OCC directly affects the operations headway. In recent years, APMs have adopted Communications-Based Train Control (CBTC) with moving block technology. This helps to shorten the headways between successive trains compared to fixed block technology. With the complex APM operations, operation planning must be detailed to ensure the possible service and train numbers needed according to the requirements for the different periods of expansion that are planned. Various factors such as operation headway, dwell time, train type, train speed, and infrastructure are related to the service operations. The feasible timetable design of the APM system is complicated. Even though there is growing literature about the APM [3, 4] and rail simulations [5–9] there has been limited study on operations simulations of the APM at the airport. This research applied microscopic simulation models to assess the APM operability based on the planned infrastructure and passenger transit requirements in each phase of airport expansion. The model helps to understand the sensitivity of the results when different parameters may be used during the actual operations.

This paper has six main sections. Section I outlines the background and problem statement, with a related

Manuscript received September 11, 2023; revised October 7, 2023; accepted October 18, 2023; published April 9, 2024.

Literature Review as Section II. Section III presents an overview of the APM case study at Suvarnabhumi Airport. Section IV presents the simulation modelling. Discussion of the results is presented in Section V. Finally, Section VI presents conclusions.

II. LITERATURE REVIEW

With the rapid growth of the aviation industry in the last two decades, most major airports have needed to expand terminal facilities. APMs are now used at many large international airports around the world to facilitate the movement of passengers between buildings and terminals. Airport APMs can be divided into two types, depending on the area divisions in the airport, namely airside and landside. Airside refers to the areas within the airport that planes use for take-off and operating areas, including buildings in these areas. These areas are considered restricted areas and have access control, or are areas where people have already passed security checks. Landside refers to the area and buildings inside the airport that are not within airside areas. These are areas without security controls, and include buildings such as the passenger terminal or parking buildings [2]. In the past, APMs were commonly used airside to connect between passenger terminals and satellite buildings. The largest airside APM was implemented at the Dallas Fort Worth International Airport, Texas, United States with a total distance of 20.9 km [10]. Nowadays, the demand for airport use is increasing and large airports have been expanding their buildings. This has resulted in the installation of APMs to provide convenient connections between passenger terminals in the landside areas.

There are several operations challenges with the driverless APM system. All vehicle or train positions need to be continuously monitored by the Operations Control Center (OCC) to maintain a safe separation distance. It requires detailed analysis of the track occupation and interactivity between different trains similar to a railway system. The APM transports high volumes of passengers in the extended airport coverage areas during a short period of time. The operations challenges are quite different from metro systems because it is a small transit system that operates in a limited area. Therefore, the headway is often limited by the physical characteristics of the rail infrastructure. With the help of simulation tools, we can model trains running under the planned infrastructure to test the feasibility of the operations timetable. However, most simulation work addresses operations improvements for freight trains [6, 11] and passenger trains [9, 12] services but not for APMs at airports. As the APM is becoming a key transport technology, especially for large airports, it is worth using a simulation to investigate the operations to ensure service viability of APM driverless operations.

In general, timetable simulation programs can be modelled at either the macroscopic or microscopic level. For a macroscopic simulation, signalling, and platform assignments may not be detailed in the model. With fewer required input parameters, the macro simulation can proceed quickly for an overview of the network level.

In contrast, the microscopic simulation has detailed input data of infrastructure, including platform assignments, and the signalling system. Train operations in a microscopic simulation will be possible only when the train occupies a block that does not overlap [13]. This takes more computational effort but the operations are in accordance with a real situation.

Overall, the maximum number of trains that can be in the network, and the line capacity, depends on technical factors such as headway, signalling, infrastructure and rolling stock; and on operations factors such as operation pattern [14], route itinerary and type of services [15–17]. Line capacity in a real operation is complex and involves a number of factors [18–20]. These include the infrastructure (single or double track, the number of platforms, platform length, distance between stations, line speed restrictions, radius, gradient, and turnout). Also to be considered is the signalling (block length and the distance between signals). The design of a signalling system is related to the track occupation of a train [21]. In addition, rolling stock information such as tractive force, numbers of engines, braking characteristics influenced train movements and line capacity in this case [19]. In order to increase the line capacity, different schemes can be used, such as reducing the dwell time, rearranging the station locations, adjusting the train speed, or installing additional signaling equipment [11, 22]. However, adjusting the dwell time affects passengers directly in terms of service satisfaction and may cause density problems on the station platform if passengers cannot board the train. Simulation models can also reproduce the situation of train operation under services disruptions and evaluate mitigation measures [14].

The microscopic simulation can help to evaluate the system line capacity [23, 24]. It can show the detailed relationships between factors that affect complex APM operations, i.e., operation headway, train type, dwell time, travel time, and rail infrastructure. These factors are directly related to the system line capacity. The simulation can modify parameters quickly to show the various effects in the system in accordance with the existing infrastructure. However, the simulation results depend on the input data and assumptions. The accuracy of the simulation results depends on the level of detail and completeness of the data. Therefore, the model must be as close to the real situation as possible in order to use the results to analyze the system precisely. The simulation model can be used to verify the APM minimum headway which is often limited by the entry-exit of the station area. This is mainly affected by the loop operations for the limited distance of the airport area [25].

III. THE OVERVIEW OF CASE STUDY

Under a recent expansion project at Suvarnabhumi Airport, a new Satellite concourse 1 (SAT-1) was constructed about 920 m away from the North Main Terminal Building (NMTB) together with an underground Automated People Mover (APM). It was initially planned that the APM would be in service to

facilitate the journeys of passengers in airside areas of the airport in mid-2022. With delays mainly due to COVID-19 this service finally came into full use in late-2023. It is designed to transport passengers between the NMTB and SAT-1 with possible expansion to an additional Satellite concourse 2 (SAT-2) and to the South Main Terminal Building (SMTB) in a later expansion phase. The expansion project can be summarized into three phases of expansion as shown in Fig. 1. Phase 2 is the connection between the North Main Terminal Building (NMTB) and the Satellite concourse 1 (SAT-1). The APM used to transport the passengers runs on four tracks that are divided into the Red Loop (RL) and Green Loop (GL). The NMTB has three platforms, which are divided into two passenger arrival platforms on the outer sides, and one departure platform in the middle. Likewise, SAT-1 has three boarding platforms with one reserved arrival platform. With three enabled platforms during normal operations, departure and arrival passengers have two equal options for boarding the trains. Phase 3 is the connection between SAT-1 and SAT-2. The distance is approximately 750 m. The APM in the third phase has only two tracks extending from the Green Loop. SAT-2 has two boarding platforms and one reserved departure platform. With two enabled platforms during normal operations, departure and arrival passengers can board the trains using the two different platforms. Phase 4 is the connection between SAT-2 and the South Main Terminal Building (SMTB). The distance is approximately 1000 m. The APM used in this phase runs on two tracks extending from the Green Loop. The SMTB has two platforms and one reserved arrival platform. With the two enabled platforms during normal operations, departure and arrival passengers can board the trains using the two different platforms.

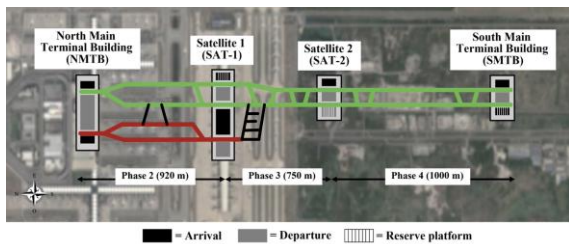


Fig. 1. The APM at Suvarnabhumi airport.

Required passenger transit capacity in terms of “Passengers per hour per direction (pphpd)” during Peak, Off-Peak and Surged Peak periods for all expansion phases is shown in Table I. The APM operates 24 h every day. The APM passenger transit volume is directly related to the aircraft loading and unloading operations during takeoff and landing. The Peak period is 16 h from 08:31 to 00:29, while the Off-Peak period is 8 h from 00:30 to 08:30. A additional Surged Peak period is a special period of high passenger usage caused by the operation services of large multiple aircraft such as the A-380. This is for approximately two hours during the Peak period. The duration of train stops at each station or “dwell time” during the Off-Peak and Peak equals 70 s, while Surged Peak equals 84 s. This is mainly affected by

the different alighting and boarding times of the passengers during the different periods.

TABLE I. THE REQUIRED PASSENGER TRANSIT CAPACITY AT DIFFERENT PERIODS

Expansion Phase	Minimum Required Capacity in Each Period			Required Dwell time	
	Off-Peak (pphpd)	Peak (pphpd)	Surged Peak (pphpd)	Off-Peak and Peak	Surged Peak
2	1,795	3,590	5,960		
3	2,717	5,435	9,022	70 s	84 s
4	4,186	8,372	10,741		

The APM train used at Suvarnabhumi Airport is the Siemens-Airval model with Married-Pair (MP) type. Each MP is a two-car train with a capacity of 210 passengers per train. The train uses a rubber-tire suspension bogie running on a concrete surface with a guidance rail in the middle and power rails to the side.

IV. METHOD

A. Model Building

In our research, we used OpenTrack 1.10.2 software to simulate the APM system in our airport case study. A simulation model was used to evaluate the feasibility of APM operations. OpenTrack is a microscopic timetable simulation that can assess train interactions with the guided way infrastructure for various operations patterns. In constructing the simulation model, the three main inputs are as follows:

1) *Guideway infrastructure*: This refers to the APM running pathway. We need to specify the pathway key characteristics such as the running length, platform length and location, gradient and radius, turnout position, and line speed restrictions. The line speed restriction when running through the radius is equal to 35 km/h; running through the gradient it equals 35 km/h; running through the turnout it is equal to 25 km/h; and running through the turnout with radius speed is equal to 15 km/h.

2) *Train/Rolling stock*: This refers to the APM vehicles that are running on the network. We need to provide the specifications of all train sets as shown in Table II. We use the Siemens-Airval model with two-cars per train known as the Married-Pair (MP) for the APM vehicles. A coupled train is possible with a maximum of four-cars per train or 2 MPs.

TABLE II. TRAIN CHARACTERISTICS

Item	Value
Train Model	Siemens-Airval
Weight	Car-A = 22.714 t, Car-B = 23.773 t
Length	Car-A = 11.2 m, Car-B = 11.2 m
Resistance equation; $F = [kN]$, $v = [m/s]$	$F = 2.338 + (0.03012v) + (0.000428v^2)$
Maximum acceleration and deceleration	1.3 m/s ²
Maximum speed	80 km/h
Number of motorized axles per car	Car-A = 1, Car-B = 2
Maximum tractive effort per motor	32.72 kN
Nominal traction effort per motorized axle [N]	Min (32715; 190000/v)

3) *Train itinerary*: This refers to the service operations of the APM system. It includes information about the route served, such as the origin, destination, stopping stations, and the timetable headway. The APM service is from the existing terminal building to the satellite terminals and the new terminal building. The train itineraries are varied according to the different expansion phases.

A simulation needs to determine the train performance. This means that under the same situation or operation route, the simulation results must be as close as possible to the real situation. In this research, the running time and average speed were used as indicators to calibrate the model. We simulated a single train running on four different lines as shown in Fig. 2. The running time and average speed results for different train performances are shown in Table III. We selected a train performance of 80% for further analysis as it results in less than 5% difference from the manufacturer information. The

simulation model was validated using the available speed data from the Phase 2 expansion between the NMTB and SAT-1 during the test running period in November 2021. The temporary line speed reductions toward the beginnings and ends of the lines are used together with the modified maximum speed of 75 km/h in the test running environment. Our simulation running times for four different lines results in less than 4% difference from the average actual running time.

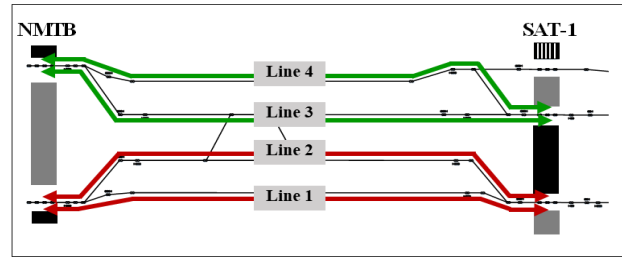


Fig. 2. Four different APM lines between NMTB and SAT-1 stations.

TABLE III. COMPARISON OF RESULTS BETWEEN THE SIMULATION MODEL AND MANUFACTURER INFORMATION

Route	Description	Manufacturer	Train performance (Simulation model)			
			100%	90%	85%	80%
Line 1	Running time from NMTB to SAT-1	116 s	105 s	111 s	116 s	122 s
	Average speed from NMTB to SAT-1	28.7 km/h	32.3 km/h	30.6 km/h	29.3 km/h	27.8 km/h
Line 2	Running time from NMTB to SAT-1	121 s	104 s	113 s	113 s	123 s
	Average speed from NMTB to SAT-1	27.6 km/h	31.8 km/h	29.3 km/h	29.3 km/h	26.9 km/h
Line 3	Running time from NMTB to SAT-1	98 s	87 s	92 s	97 s	100 s
	Average speed from NMTB to SAT-1	34 km/h	38.1 km/h	36 km/h	34.1 km/h	33.1 km/h
Line 4	Running time from NMTB to SAT-1	135 s	117 s	126 s	130 s	138 s
	Average speed from NMTB to SAT-1	24.7 km/h	28.3 km/h	26.3 km/h	25.5 km/h	24.0 km/h

B. Scenario Design

The scenario planning of this model is based on the three different periods for each phase of operations. The required passenger transit capacity was transformed into the required operations headway based on the APM capacity of 210 passengers per train (1 MP). For example, in Phase 2 during Off-Peak time, the passenger demand or “required capacity” is 1,795 passengers per hour per direction (pphpd). The number of trips in an hour can be

calculated using 1,795 divided by 210 which equals 8.55 trips/hour. Therefore, the train must operate between NMTB and SAT-1 for at least 8.55 trips per direction in one hour. The required headway can be calculated using 3,600 s divided by 8.55 which is equal to 421.05 s. The train must operate at the maximum headway or “required headway” of 421.05 s to accommodate all passenger demand. The scenario planning of this research can be summarized in Table IV.

TABLE IV. SCENARIO PLANNING OF THIS RESEARCH

Phase	Periods	Required Capacity	Number of Trips/hour	Required Headway	Required Dwell Time
2 (NMTB-SAT-1)	Off-Peak	1,795 pphpd	1795/210 = 8.55	421.05 s	70 s
	Peak	3,590 pphpd	3590/210 = 17.10	210.53 s	
	Surged Peak	5,960 pphpd	5690/210 = 28.38	126.85 s	84 s
3 (NMTB-SAT-2)	Off-Peak	2,717 pphpd	2717/210 = 12.94	278.21 s	70 s
	Peak	5,435 pphpd	5435/210 = 25.88	139.10 s	
	Surged Peak	9,022 pphpd	9022/210 = 42.96	83.80 s	84 s
4 (NMTB-SMTB)	Off-Peak	4,186 pphpd	4186/210 = 19.93	180.63 s	70 s
	Peak	8,372 pphpd	8372/210 = 39.87	90.76 s	
	Surged Peak	10,741 pphpd	10741/210 = 51.15	70.38 s	84 s

Initially, the simulation model is divided into two parts. The first part is to simulate the model as a single train, to study and analyze the running time of each route. This includes evaluating the turn-back operations at the entry-exit areas of the stations. The second part is to simulate multiple trains in the overall network at each phase of the expansion. Based on the required capacity, the operations configurations are determined. The feasible headway together with the running time and capacity performance are reported in Table IV. Station dwell time may need to be adjusted to avoid conflicts at station entry-exit areas. The train running time is evaluated and compared with the single train running time to see if there is any delay or additional running time in the network due to high traffic volume.

V. RESULT AND DISCUSSION

A. Model Building

1) Single train simulation

The MP train running times for different phases of operations without dwell time are summarized in Fig. 3. In Phase 2, the running time on the Red Loop is 248 (125+123) s and Green Loop is 250 (124+126) s. In the

combined expansion of Phases 2 and 3, the running time of the Green Loop is 365 (124+61+58+122) s. For the full expansion of Phases 2–4, the running time of the Green Loop is 519 (124+56+83+76+58+122) s.

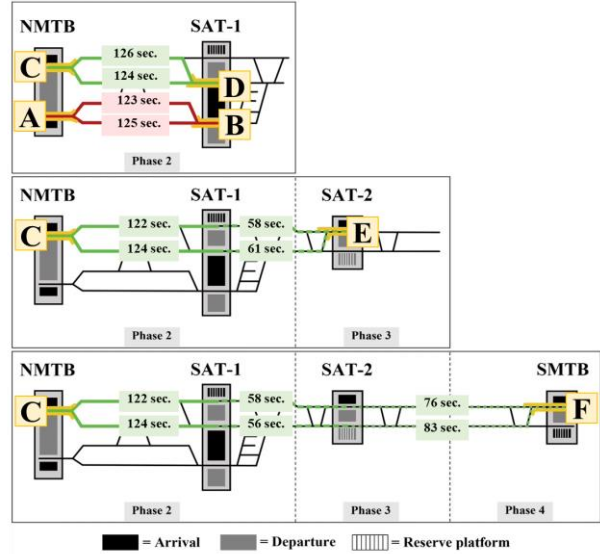


Fig. 3. Running time of each phase.

TABLE V. THE ENTRY-EXIT TRAIN PATH RESERVING TIME

Phase	Area	Periods	Train path reserving without dwell time	Train path reserving with dwell time	
2	A (NMTB)	Off-Peak and Peak	24 + 26 = 50 s	24 + 70 + 26 = 120 s	
		Surged Peak		24 + 84 + 26 = 134 s	
	B (SAT-1)	Off-Peak and Peak	28 + 27 = 55 s	28 + 70 + 27 = 125 s	
		Surged Peak		28 + 84 + 27 = 139 s	
	C (NMTB)	Off-Peak and Peak	24 + 26 = 50 s	24 + 70 + 26 = 120 s	
		Surged Peak		24 + 84 + 26 = 134 s	
3	D (SAT-1)	Off-Peak and Peak	28 + 27 = 55 s	28 + 70 + 27 = 125 s	
		Surged Peak		28 + 84 + 27 = 139 s	
	E (SAT-2)	Off-Peak and Peak	39 + 36 = 75 s	39 + 70 + 36 = 145 s	
		Surged Peak		39 + 84 + 36 = 159 s	
	4	F (SMTB)	Off-Peak and Peak	39 + 36 = 75 s	39 + 70 + 36 = 145 s
			Surged Peak		39 + 84 + 36 = 159 s

A bottleneck of the APM system occurs at the turn-back stations. The APM performs the turn-back using a single track operation at the entry-exit of the station. The entry-exit positions of all stations are shown by the letters A-F in Fig. 3. When the preceding train enters and stops at the station, it affects the following train which cannot enter the station. The following train can enter the station only when the preceding train has left. This requires proper train separation distance between the two trains so that the “blocking time” of the two trains does not overlap. The train blocking time is the reserve time for each train path in the operation [15]. Table V summarizes the station entry-exit blocking time from each phase of operation using the 1 MP train for all six station areas (A–F). The NMTB station turnaround area is at point A for the Red Loop and C for the Green Loop. For the SAT-1 station, the turnaround area is at point B for the Red Loop and D for the Green Loop. The SAT-2 and SMTB turn around areas are respectively at Points E and F. The train path reserving time for each station area is composed of three blocking times including the interval

time of the train occupying a block section before arrival at the station, the dwell time at the station, and the interval time of the train occupying a block section when departing the station.

2) Network train simulation

The feasible operation configurations are determined under the multiple train simulation environment. In a real situation, to accommodate the number of passengers, the APM system may not be able to operate with very short headway. This is due to the turn-around operation at the entry-exit of each station area. In our study, there are two major approaches that can increase line capacity to accommodate high passenger transit requirements. The first is to decrease the headway to be not lower than the blocking time limit at the entry-exit of the turn-around station. Another way is to increase train capacity by using coupled trains to accommodate more passengers per trip. When encountering the route conflicts, adjusting the train speed by slowing down or adjusting the station dwell time may be needed. However, doing so will affect the trip time and the number of trains needed.

Table VI summarizes the results for the three different phases of airport expansion. If it is not possible to operate the train according to the required headway, then the APM operation will be adjusted to a simulation headway. If the required capacity cannot be achieved under the 1 MP train configuration, the coupled train of the 2 MP configuration is used. Based on the specific train configuration, simulation headway, and pre-specified dwell time, the train running time can be reported as part of the simulation results. The number of trips and trains can be determined. The passenger transit capability is then determined by comparing the simulation capacity versus the required capacity. This is reported as “capacity performance”. In some cases, different parameter values may be suggested in order for the train to operate without conflicts or delays. Different dwell times may be used for

sensitivity analysis to reflect the possible alternative solutions. However, the selected dwell time must be sufficient for passenger boarding and alighting in practice.

To increase line capacity, headway should be decreased or train capacity should be increased. Train capacity can be adjusted using either the uncoupled train of a MP (2-car) or a coupled train of a MP (4-car). The operations headway is often constrained by the blocking time at the entry-exit station areas (see Table V). Due to the train operating on the single track in that area, only one train can operate at a time. When encountering route conflicts, some train routes should be modified to avoid conflicts, for example adjusting the train speed by slowing down or adjusting the station dwell time to avoid the conflicts. However, doing so will affect the trip time and the number of trains.

TABLE VI. SIMULATION RESULTS OF NETWORK TRAINS

Phase	Period	Required Headway	Scenario	Simulation Headway	Operation headway at station	Dwell time	Running time without dwell time (round trip)	Number of trips from NMTB /to NMTB (per direction per hour)	Number of trains	Capacity performance (%)
2	Off-Peak	421.05 s	2.1	420 s (RL)	420 s	<u>70-85 s</u>	248 s	9 / 9	1-1 MP	$(9 \times 210) / 1795 = 105.3\%$
	Peak	210.53 s	2.2	200 s (RL)	200 s	70 s	248 s	18 / 18	2-1 MP	$(18 \times 210) / 3590 = 105.3\%$
			2.3	250 s (RL)	250 s		251s (4C)	15 / 15	2-2 MP	$(15 \times 420) / 5960 = 105.7\%$
	Surged Peak	<u>126.85 s</u>	2.4	250 s (RL) 250 s (GL)	125 s	<u>84-125 s</u>	248 s 250 s	29 / 29	4-1 MP	$(29 \times 210) / 5960 = 102.2\%$
3	Off-Peak	278.21 s	3.1	250 s (GL)	250 s	<u>70-95 s</u>	365 s	14 / 13	3-1 MP	$(14 \times 210) / 2717 = 108.2\%$ (NMTB-SAT2) $(13 \times 210) / 2717 = 100.5\%$ (SAT2-NMTB)
			3.2	250 s (GL)	250 s	<u>70-95 s</u>	371 s (4C)	14 / 13	3-2 MP	$(14 \times 420) / 5435 = 108.2\%$ (NMTN-SAT2) $(13 \times 420) / 5435 = 100.5\%$ (SAT2-NMTB)
	Peak	<u>139.10 s</u>	3.3	135 s (GL)#	135 s	70 s	467 s (TB)	28 / 25	6-1 MP	$(28 \times 210) / 5435 = 108.2\%$ (NMTB-SAT2) $(25 \times 210) / 5435 = 96.6\%$ (SAT2-NMTB)
			3.4	165 s (GL)	165 s	<u>70 s</u>	371 s (4C)	22 / 22	4-2 MP	$(22 \times 420) / 9022 = 102.4\%$ $(22 \times 420) / 9022 = 102.4\%$ (NMTB-SAT2)
			3.5	165 s (GL)	165 s	<u>84-90 s</u>	454 s (4C+)	22 / 20	5-2 MP	$(20 \times 420) / 9022 = 93.1\%$ (SAT2-NMTB)
	Surged Peak	<u>83.80 s</u>	3.5	165 s (GL)	165 s	<u>84-90 s</u>	454 s (4C+)	22 / 20	5-2 MP	$(20 \times 210) / 4186 = 100.3\%$ (NMTB-SMTB) $(17 \times 210) / 4186 = 85.3\%$ (SMTB-NMTB)
	4	Off-Peak	180.63 s	4.1	180 s (GL)	180 s	<u>60 s</u>	519 s	20 / 17	5-1 MP
4.2				180 s (GL)	180 s	<u>70-80 s</u>	609 (+)	20 / 20	6-1 MP	$(20 \times 210) / 4186 = 100.3\%$
4.3				160 s (GL)	160 s	70 s	519 s	22 / 22	6-1 MP	$(22 \times 210) / 4186 = 115.4\%$
4.4				160 s (GL)	160 s	70 s	525 s (4C)	22 / 22	6-2 MP	$(22 \times 420) / 8372 = 115.4\%$
Peak		<u>90.76 s</u>	4.5	180 s (GL)	180 s	<u>70-80 s</u>	618 s (4C+)	20 / 20	6-2 MP	$(20 \times 420) / 8372 = 100.3\%$
			4.6	180 s (GL) 250 s (RL)	180 s 250 s	84 s	525 s (4C) 251 s (4C)	35 / 35 20(GL) + 15(RL)	6-2 MP 2-2 MP	$(35 \times 420) / 10741 = 136.8\%$ (GL+RL) $(20 \times 420) / 10741 = 78.2\%$ (GL Only)
			4.7	130 s (GL)#	130 s	NMTB, SAT-1, SAT-2 = <u>80 s</u> SMTB = <u>100 s</u>	525 s (4C)	28 / 24	8-2 MP	$(28 \times 420) / 10741 = 109.5\%$ (NMTB-SMTB) $(24 \times 420) / 10741 = 93.8\%$ (SMTB-NMTB)

Notes: 1) Dash underline (____) means the train cannot operate according to the required headway.

2) Pound (#) means opening the additional platform at the end terminal.

3) Solid underline (___) means the dwell time is less than the required dwell time. Double Solid underline (____) means the dwell time is more than the required dwell time.

4) 4C means additional running time caused by using 4 car trains when compared to the 1MP train running time.

5) Plus (+) means additional running time when compared to the 1MP or 2MP single train simulation.

6) TB means the train turned back beyond SAT-2 station.

In Phase 2, the train can operate according to the required headway except during Surged Peak, because it is limited by blocking time at points A, B, C, and D (see Table V). Therefore, the headway that can be operated was recalculated. This can be adjusted in two ways. The first is to couple the train to the 2 MPs and a new headway of 250 s is determined. In this case, the train running time is 251 s: a 3 s increase when compared to the 1 MP train running time of 248 s (see Scenario 2.3 in Table VI). Another way is to use the MP train type and operate on the Red Loop and Green Loop, with headway on each loop of 250 s. Both loops can allow the train to be released alternately. It will have headway at the station equal to 125 s (see Scenario 2.4 in Table VI). With both methods, the train can stop at the station for approximately 84–125 s. In this phase, the number of MPs required for service is up to four trains.

In Phase 3 the simulation result shows that during Peak times, the train cannot operate at the required headway because it is limited by blocking time at point E (see Table V). Therefore, the headway that can be operated was recalculated and the train was adjusted to the 2 MPs train type. The new headway is 250 s and the dwell time approximately 70–95 s. In this case, the train running time is 371 s: a 6 s increase when compared to the 1 MP train running time of 365 s (see Scenario 3.2 in Table VI). In addition, it can be seen that the train route can be modified to a new route by making a turn back beyond the SAT-2 station and opening three platforms as shown in Fig. 4. For the modified turn back operation, all three platforms should be used at SAT-2. In these circumstances, it can operate at headway of 135 s with 70 s dwell time. This is close to the required headway, but it increases the running time to 467 s (see Scenario 3.3 in Table VI).

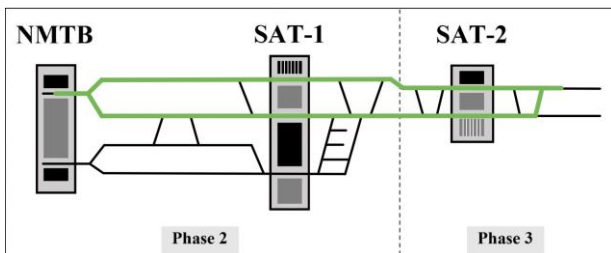


Fig. 4. The Phase 3 operation with the turn back beyond SAT-2 station.

In Phase 3, the required headway during Surged Peak is high compared with the critical blocking time. Therefore, the simulation is adjusted to use the 2 MPs train type and the headway of 165 s is recalculated in order to satisfy the transit requirement. However, the headway of 165 s causes a delay with the fifth train at the NMTB station as shown in Fig. 5. This can be adjusted in two ways. The first is to reduce the dwell time at all stations from 84 s to 70 s and adjusting the train to the 2 MPs train type. In this case, the train running time is 371 s: a 6 s increase when compared to the 1 MP train running time of 365 s (see Scenario 3.4 in Table VI). Another way is to reduce the train speed in the direction of the SAT-1 to NMTB. This increases the running time

to 454 s (see Scenario 3.5 in Table VI). In this phase, the number of MPs required for service is increased to ten trains.

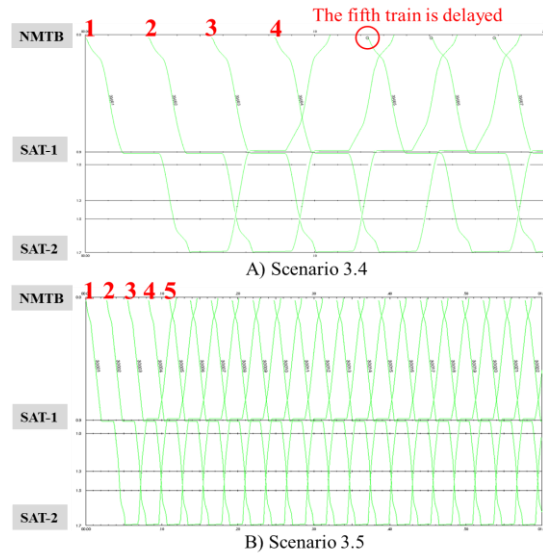


Fig. 5. Train diagram of Phase 3 during the Surged Peak.

In Phase 4 the simulation result shows that during Off-Peak, trains can operate according to the required headway, but there is a conflict at the NMTB station: the same for Phase 3 during Surged Peak. This can be adjusted in three different ways. The first is to reduce the dwell time at all stations from 70 s to 60 s (see Scenario 4.1 in Table VI). The second way is to reduce the train speed in the direction of SAT-1 to NMTB. This increases the running time to 609 s and dwell time to approximately 70–80 s (see Scenario 4.2 in Table VI). The third way is to use a headway of 160 s and adjust dwell time to 70 s (see Scenario 4.3 in Table VI). This prevents train conflicts by letting the train depart the NMTB station earlier: before the other train arrives at NMTB. The latter two ways will use more trains than the first way. During Peak times, the train cannot operate according to the required headway because it is limited by blocking times at points C and F (see Table V). Therefore, the train is adjusted to the 2 MPs train type to accommodate more passengers. This can be adjusted in two ways. The first is to adjust the headway to 160 s and dwell time equal to 70 s. In this case, the train running time is 525 s: a 6 s increase when compared to the 1 MP train running time of 519 s (see Scenario 4.4 in Table VI). The other way is determining headway at 180 s and dwell time at approximately 70–80 s. This increases the running time to 618 s (see Scenario 4.5 in Table VI). Both ways use the same number of trains, but with different headway and dwell times. During Surged Peak, the required headway is tight. The train cannot operate at the required headway even with the 2 MPs train type. There are two possible options for operation in order to satisfy the transit requirements. The first is to run an additional short loop operation using the Red Loop in addition to the Green Loop, even though the Red Loop operation can only transport passengers between NMTB and SAT-1 and

not the full loop like the Green Loop. Under this scheme, the Red Loop headway is 250 s and 180 s for the Green Loop. In this case, the train running time using the 2 MPs train for the Green Loop is 525 s and the Red Loop is 251 s (see Scenario 4.6 in Table VI). With the second solution, the SMTB station should operate with all three platforms at a headway of 130 s. However, the dwell times at NMTB, SAT-1 and SAT-2 are changed to 80 s and the dwell time at SMTB is changed to 100 s (see Scenario 4.7 in Table VI). This is to avoid conflicts at the entry-exit of the station. In this phase, the number of MPs required for service is increased to sixteen trains.

VI. CONCLUSION

As the Automated People Mover (APM) is becoming key transportation technology at major airports to transport high volumes of passengers in a short period of time, APM operations must be planned to ensure service capability. A microscopic simulation model has therefore been constructed to ensure the safety of driverless operations and give some operations insights into the different phases of airport expansion. As the bottleneck of the APM system occurs at the turn-back stations, the entry-exit train path reserving time was first investigated. Feasible APM timetable and operation configurations were determined using a multiple train simulation environment. To avoid route conflicts in the entry-exit areas caused by the high traffic volumes, the station dwell times or train speeds need to be adjusted which may result in additional train running time. Based on our study, the simulation model shows the detailed relationships between the various factors that affect complex APM operations, such as operations headway, rail-car availability, dwell time, travel time, and rail infrastructure. A coupled train with two married pairs (4-car) can accommodate more passengers resulting in higher train capacity. The headway can be decreased within certain limits to achieve the benefits of higher network capacity.

As for the operations during the Off-Peak period for all three phases of airport expansion, the uncoupled-trains can be used to fulfill the transit requirement. However, additional travelling time or modified dwell time is required to avoid conflicts in the entry-exit station areas due to high traffic volumes in Phase 4. During the Peak period, use of the uncoupled train is still possible only for Phases 2 and 3. For Phase 3 Peak period with an uncoupled train, the turn-around location needs to be moved beyond the station to reduce the traffic volume in the entry-exit area of SAT-2 station. However, the travelling time is not compromised if we use coupled trains. For Phase 2 Surged Peak period, both Red Loop and Green Loop need to operate uncoupled trains. If only one loop is implemented, coupled trains should be used. For the Phase 3 Surged Peak, additional travelling time or adjusted dwell time is required to avoid conflicts in the entry-exit station areas due to high traffic volume. For the Phase 4 Surged Peak, the transit requirements can be achieved either by using only the Green Loop or both Red Loop and Green Loop. If only the Green Loop is

used, dwell time at all stations needs to be adjusted to prevent conflicts in the entry-exit areas of the stations. The opening of the reserved platform is needed to shorten the headway time.

In our study, the transit requirement was estimated before the construction of the airport expansion. Even though it is insightful to plan ahead, adjustments may be needed as demand is realized. However, the various factors that affect complex APM operations are still valid and can be investigated using the existing simulation model. For future research directions, it will be interesting to investigate the resilience and robustness of the timetable under the service disruptions and delays after full operations are realized at the airport. In addition, it is worthwhile investigating the different power consumption for different service patterns.

CONFLICT OF INTEREST

The authors declare no conflict of interest.

AUTHOR CONTRIBUTIONS

Wareesara Weerawat set up this research topic and the guidance for the simulation analysis. Taksaporn Thongboonpian constructed and ran the model. Norio Tomii give advice on writing this paper. All authors had approved the final version.

FUNDING

This research was partially supported by both the European Union's Horizon 2020 Research and Innovation programme RISE under grant agreement no. 823759 (REMESH) and the Thailand Science Research and Innovation (TSRI) under the Research and Researchers for Industries (RRI) project.

ACKNOWLEDGMENT

We would like to thank Mr. Ditsapol Padungkul, Managing Director of Reung Narong Co., Ltd, for the APM technical data and the partial sponsorship of this research. We would like to thank Mr. Graham Rogers for his suggestions on improving the English.

REFERENCES

- [1] Suvarnabhumi Airport. *Wikipedia*. [Online]. Available: https://en.wikipedia.org/w/index.php?title=Suvarnabhumi_Airport&oldid=1176248705
- [2] People mover. *Wikipedia*. [Online]. Available: https://en.wikipedia.org/w/index.php?title=People_mover&oldid=1173419651
- [3] F. C. Barbosa, "Automated people mover technology review—A mobility tool for large capacity airports and connecting transit systems," in *Proc. the 2022 Joint Rail Conference*, 2022. <https://doi.org/10.1115/JRC2022-78132>
- [4] M. van Doorne, G. Lodewijks, and W. B. van Blokland, "Adapting automated people mover capacity on airports to real time demand," in *Proc. the 23rd World Conference Air Transport Research Society (ATRS 2019)*, 2019.
- [5] W. Weerawat, L. Samitwintikul, and R. Torpanya, "Operational challenges of the bangkok airport rail link," *Urban Rail Transit*, vol. 6, no. 1, pp. 42–55, 2020. <https://doi.org/10.1007/s40864-019-00121-3>

- [6] E. Tischer, P. Nachtigall, and J. Široký, “The use of simulation modelling for determining the capacity of railway lines in the Czech conditions,” *Open Engineering*, vol. 10, no. 1, pp. 224–231, 2020. <https://doi.org/10.1515/eng-2020-0026>
- [7] S. Harrod, F. Cerreto, and O. A. Nielsen, “OpenTrack simulation model files and output dataset for a Copenhagen suburban railway,” *Data in Brief*, vol. 25, 103952, 2019. <https://doi.org/10.1016/j.dib.2019.103952>
- [8] R. Haehn, E. Ábrahám, and N. Nießen, “Probabilistic simulation of a railway timetable,” in *Proc. the 20th Symposium on Algorithmic Approaches for Transportation Modelling, Optimization, and Systems (ATMOS 2020)*, Schloss Dagstuhl-Leibniz-Zentrum für Informatik, 2020.
- [9] P. Potti and M. Marinov, “Evaluation of actual timetables and utilization levels of west midlands metro using event-based simulations,” *Urban Rail Transit*, vol. 6, pp. 28–41, 2020. <https://doi.org/10.1007/s40864-019-00120-4>
- [10] List of airport people mover systems. *Wikipedia*. [Online]. Available: https://en.wikipedia.org/w/index.php?title=List_of_airport_people_mover_systems&oldid=1176219432
- [11] I. Ljubaj, M. Mikulčić, and T. J. Mlinarić, “Possibility of increasing the railway capacity of the R106 regional line by using a simulation tool,” *Transportation Research Procedia*, vol. 44, pp. 137–144, 2020. <https://doi.org/10.1016/j.trpro.2020.02.020>
- [12] M. Khodaparastan, O. Dutta, M. Saleh, and A. A. Mohamed, “Modeling and simulation of DC electric rail transit systems with wayside energy storage,” *IEEE Transactions on Vehicular Technology*, vol. 68, no. 3, pp. 2218–2228, March 2019. doi: 10.1109/TVT.2019.2895026
- [13] J. Pachl, “Railway signalling principles,” *Braunschweig*, June 2020. <https://doi.org/10.13140/RG.2.2.14777.60004/1>
- [14] Y. Zhu and R. M. Goverde, “Railway timetable rescheduling with flexible stopping and flexible short-turning during disruptions,” *Transportation Research Part B: Methodological*, vol. 123, pp. 149–181, 2019. <https://doi.org/10.1016/j.trb.2019.02.015>
- [15] Z. Liao, H. Li, J. Miao, and F. Corman, “Railway capacity estimation considering vehicle circulation: Integrated timetable and vehicles scheduling on hybrid time-space networks,” *Transportation Research Part C: Emerging Technologies*, vol. 124, 102961, 2021. <https://doi.org/10.1016/j.trc.2020.102961>
- [16] T. Rosberg and B. Thorslund, “Simulated and real train driving in a lineside Automatic Train Protection (ATP) system environment,” *Journal of Rail Transport Planning & Management*, vol. 16, 2020. <https://doi.org/10.1016/j.jrtpm.2020.100205>
- [17] A. Shahabi, S. Raissi, K. Khalili-Damghani, and M. Rafei, “Designing a resilient skip-stop schedule in rapid rail transit using a simulation-based optimization methodology,” *Operational Research*, vol. 21, no. 3, pp. 1691–1721, 2021. <https://doi.org/10.1007/s12351-019-00523-y>
- [18] M. K. Sameni and A. Moradi, “Railway capacity: A review of analysis methods,” *Journal of Rail Transport Planning & Management*, vol. 24, 100357, 2022. <https://doi.org/10.1016/j.jrtpm.2022.100357>
- [19] I. Ljubaj and T. J. Mlinarić, “The possibility of utilising maximum capacity of the double-track railway by using innovative traffic organisation,” *Transportation Research Procedia*, vol. 40, pp. 346–353, 2019. <https://doi.org/10.1016/j.trpro.2019.07.051>
- [20] N. Weik, J. Warg, I. Johansson, M. Bohlin, and N. Nießen, “Extending UIC 406-based capacity analysis—New approaches for railway nodes and network effects,” *Journal of Rail Transport Planning & Management*, vol. 15, 100199, 2020. <https://doi.org/10.1016/j.jrtpm.2020.100199>
- [21] U. Cansu, K. Atieh, and R. Stefano, “Influence of signalling systems on the capacity of railways by lines and nodes assessment methods,” *Transp. Res. Procedia*, vol. 69, pp. 321–327, 2023. <https://doi.org/10.1016/j.trpro.2023.02.178>
- [22] Z. Abdullaev, M. Rasulov, and M. Masharipov, “Features of determining capacity on double-way lines when passing high-speed passenger trains,” in *Proc. E3S Web of Conferences*, EDP Sciences, 2021, vol. 264, 05002. <https://doi.org/10.1051/e3sconf/202126405002>
- [23] N. Limboonngam and W. Weerawat, “Mixed traffic timetable simulation analysis: A case study of red line commuter train,” in *Proc. the 10th International Conference on Operations and Supply Chain Management*, 2020.
- [24] A. Shahabi, S. Raissi, K. Khalili-Damghani, and M. Rafei, “An event-driven simulation-optimisation approach to improve the resiliency of operation in a double-track urban rail line,” *Journal of Simulation*, pp. 1–20, 2021. <https://doi.org/10.1080/17477778.2021.1876535>
- [25] T. Thongboonpian and W. Weerawat, “Analysis of automated people mover operations at Suvarnabhumi airport,” *Thai Journal of Operations Research*, vol. 10, no. 2, pp. 63–71, 2022.

Copyright © 2024 by the authors. This is an open access article distributed under the Creative Commons Attribution License (CC BY-NC-ND 4.0), which permits use, distribution and reproduction in any medium, provided that the article is properly cited, the use is non-commercial and no modifications or adaptations are made.